DESIGN, FABRICATION, AND TESTING OF A MOVING MAGNET ACTUATOR FOR LARGE RANGE NANOPOSITIONING

David B. Hiemstra, Gaurav Parmar, Yi Chen, and Shorya Awtar
Precision Systems Design Laboratory, Mechanical Engineering
University of Michigan, Ann Arbor, MI 48109

ABSTRACT

Moving magnet actuators are promising candidates for achieving nanometric motion quality over a large (10mm) motion range. Large range nanopositioning capability addresses an important instrumentation need in several areas of nanotechnology. In pursuit of this goal, we present an optimal moving magnet actuator design integrated with a double parallelogram flexure bearing and thermal management system. The proposed design is systematically optimized in the context of fundamental actuation- and system-level performance trade-offs that we have identified. The overall system is custom-fabricated and tested to validate the desired actuation performance. Preliminary closed-loop results highlight the proposed actuator's potential for large range nanopositioning.

INTRODUCTION AND MOTIVATION

Large range (~ 10 mm) nanopositioning systems are becoming increasingly desirable in applications such as scanning probe microscopy, nanometrology, nanolithography, hard-drive and semiconductor inspection, and memory storage [1-2]. However, most existing nanopositioning systems are generally limited to a motion range of a few hundred microns [2-3], in part due to actuation challenges. The voice coil actuator (VCA), which is a single-phase electromagnetic actuator, has stood out among other options such as piezoelectric, inchworm-type, and multi-phase electromagnetic actuators, for its non-contact, frictionless and cog-free motion characteristics and sufficient motion range suitable for large range nanopositioning [4-5]. However, in a VCA, the non-deterministic disturbance due to the moving connecting wires and heat dissipation from the coil connected to the motion stage degrade the overall motion quality (resolution, precision and accuracy).

While the operation of a moving magnet actuator (MMA) is similar to that of a VCA, its construction is different in that it employs non-moving coils and a moving magnet. FIGURE 1

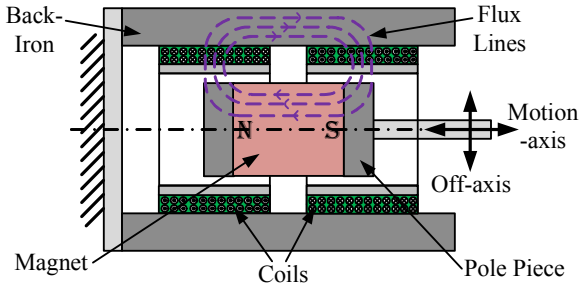

FIGURE 1. Moving Magnet Actuator Schematic.

illustrates a traditional MMA configuration, featuring an axially-oriented cylindrical magnet and iron pole pieces that are connected to the motion stage of the bearing, which serve as the "mover". The "stator" consists of a tubular back-iron, along with two oppositely wound coils that are connected in series. This configuration gives MMAs two distinct advantages over the VCA: **I.** The non-deterministic disturbance due to the moving cables is eliminated, making MMAs truly non-contact actuators. **II.** Since the coils are connected to the static back-iron as opposed to the mover, the heat generated due to resistive losses in the coils remains physically separated from the motion stage. Given these attributes, MMAs are promising candidates for large range nanopositioning.

The objective of this research is to systematically develop and demonstrate an optimal MMA design that takes into account **I.** Physical performance trade-offs, as described further below, and **II.** MMA-specific challenges including greater non-uniformity in force over stroke and off-axis instability of the mover [6].

PERFORMANCE TRADE-OFFS

An MMA, double parallelogram flexure bearing, and thermal management system were concurrently designed to meet the following system-level performance criteria: **I.** Maximize the first natural frequency (or open-loop bandwidth) since this is closely related to the achievable speed and disturbance rejection of the motion system in closed-loop operation. **II.** Minimize the power consumption of the actuator

and effectively dissipate the generated heat, which is detrimental to the motion system's performance. **III.** Maximize the uniformity of force with respect to position over the motion range (i.e., actuator stroke), since non-uniformities can compromise the closed-loop tracking performance of the motion system. **IV.** Ensure that the bearing counteracts any off-axis attraction between the mover and the back-iron to prevent the mover from pulling in sideways to the stator.

Simultaneously satisfying all of these criteria without any physical limits is not possible, however; for example, the force output of an MMA can be increased by either increasing the moving mass or by increasing the quasi-static power limit, both of which are undesirable. To quantitatively determine these trade-offs, a lumped-parameter model has been developed [7], which shows that for the traditional actuator configuration of FIGURE 1, the actuation force (F) remains directly proportional to the square root of the actuator moving mass (m_a) and the square root of power consumed (P), irrespective of the geometric size of the actuator. This may be expressed as:

$$\frac{F}{\sqrt{P}\sqrt{m_a}} = \frac{K_t}{\sqrt{R}\sqrt{m_a}} = \beta \ (constant),$$

where K_t is the force constant and R is the coil resistance. When employed in a flexure bearing-based motion system, an important consequence of the above relation is that it places a limit on the overall open-loop bandwidth (ω_n), given a desired motion range (Δ), power consumption limit (P_{max}), and mass of the motion stage (m):

$$\omega_n^2 < \beta \frac{\sqrt{P_{\max}}}{\Delta} \frac{\sqrt{m_a}}{m + m_a}$$

This, in turn, limits the achievable bandwidth and disturbance rejection (and therefore positioning resolution) in a closed-loop setup [8].

MMA DESIGN AND FABRICATION

As shown above, it is evident that in order to maximize the open-loop bandwidth of the motion system based on an MMA and flexure bearing, one has to maximize the constant β while keeping the moving mass as small as possible. In this work, the motion range was set to be

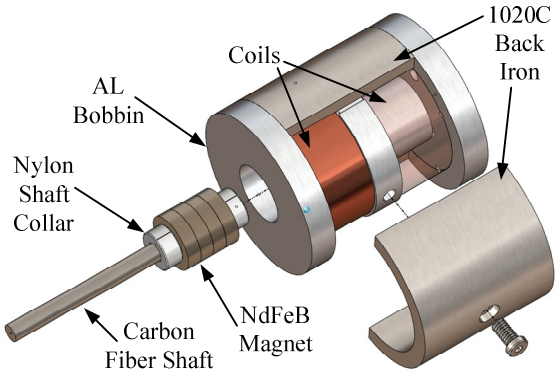

FIGURE 2. Exploded View of the MMA.

±5mm, with a power and voltage limit of 20W and 25V, respectively, based on a custom-made low noise drive amplifier and the capability of the thermal management system (described later).

The geometric design of the MMA (i.e., dimensions of the magnet, back-iron, and coil) was then carried out in a systematic manner to maximize β and minimize the moving mass [7]. This resulted in the following actuator specifications: force constant of 30N/A, actuator moving mass of 106g, coil resistance of 43Ω, force-stroke non-uniformity less than 9%, and a β value of 14√Hz.

Based on this design, a prototype of the MMA was fabricated and assembled. The components of the prototype are shown in an exploded view in FIGURE 2. A Neodymium-Iron-Boron (Grade N52) axial magnet was selected for its high remanent magnetization (1.45T), which provides a high force constant. The magnet is maintained below its Curie temperature (80°C) via a thermal management system, as described later. To minimize the moving mass, the magnet is mounted on a hollow carbon fiber shaft using Nylon sleeve collars. The coil was wound using 25AWG copper wire on an Aluminum bobbin. AL6061 was chosen for its good machinability and high thermal conductivity, and it also acts as a shorted turn, which reduces the coil inductance. The back-iron, turned from 1020C steel, exhibits a high saturation flux density of 1.6T. Additionally, it was designed as two symmetric halves so that the rest of the actuator can first be easily assembled without being affected by the strong permanent magnet field.

THERMAL MANAGEMENT SYSTEM

To make sure that the heat generated by the MMA coils will not adversely affect the

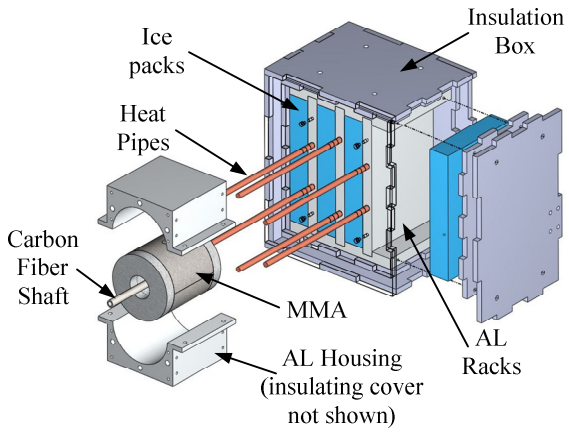

FIGURE 3. Thermal Management System.

remanence of the permanent magnet, cause distortions in the flexure bearing, or compromise the accuracy of the position sensor, a passive thermal management system (TMS) was designed and incorporated with the actuator, as shown in FIGURE 3. It provides an effective way to transfer heat from the MMA coils to an ice sink via heat pipes. This method is advantageous as compared to other convective heat dissipation methods, which may lead to air flow-induced vibrations.

A lumped-parameter thermal network model was developed to evaluate the steady-state temperature of the coil bobbin. Using this, the critical components of the TMS (heat pipes, ice packs, and Aluminum racks) were designed in order to ensure that the steady-state coil bobbin temperature remains near room temperature for at least 4 hours of operation under constant 20W power input to the actuator. The experimental results of the TMS under these conditions are shown in FIGURE 4.

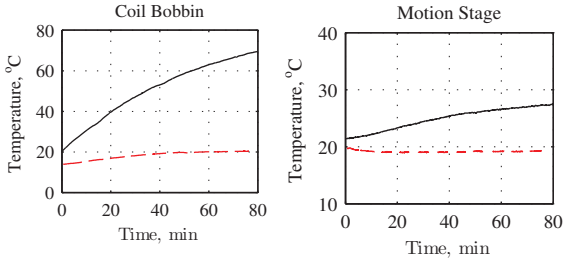

FIGURE 4. Temperature Rise with (- -) and without (—) Thermal Management System.

BEARING DESIGN AND FABRICATION

A single-axis symmetric double-parallelogram flexure bearing (FIGURE 5) was selected to provide motion guidance for the MMA for its

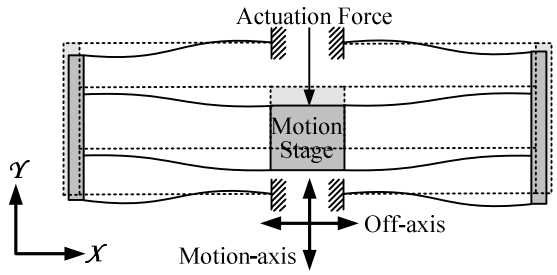

FIGURE 5. Symmetric Double Parallelogram Flexure Bearing.

linear motion direction stiffness, relatively high off-axis stiffness, and frictionless and backlash-free motion. The translational stiffness of the flexure bearing in the motion direction (K_y), in-plane off-axis direction (K_x) and out-of-plane off-axis direction (K_z) are given by:

$$K_y \approx \frac{WT^3E}{L^3};\quad K_x \approx \frac{WTE}{L};\quad K_z \approx \frac{W^3TE}{L^3}$$

where E is the Young's modulus of the material, and W, T and L are the width, thickness and length of the beam, respectively.

The minimum beam thickness and maximum beam depth were limited by the capability of the water-jet machining process and were set to be 0.75mm and 25.4mm, respectively. The beam length was chosen to be 80mm to provide a ±5mm motion range with a motion direction stiffness of 3.43N/mm. With AL6061 as the bearing material, the factor of safety against yield was estimated to be 3.96.

The negative (destabilizing) stiffness of the off-axis force between the magnet and the back-iron was calculated via FEA to be 1.3N/mm near the nominal equilibrium position, and the positive (stabilizing) stiffness of the bearing in the X- and Z-directions was found to be 149.6N/mm and 70.6N/mm, respectively, thereby ensuring the off-axis stability of the MMA.

EXPERIMENTAL SETUP

The single-axis motion system prototype, comprising the MMA, flexure bearing, and thermal management system, is shown in FIGURE 6. A custom-made current driver was built to provide direct control of the actuation force. An off-the-shelf linear optical encoder (5nm resolution) was used for position measurement and feedback. The system was

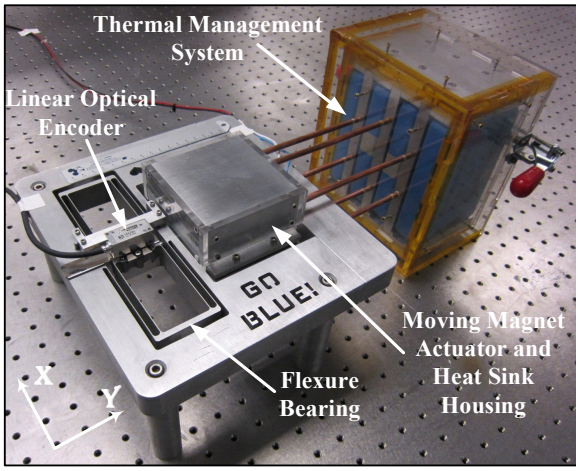

FIGURE 6. Nanopositioning System Prototype.

tested to demonstrate a 36Hz open-loop bandwidth as shown in FIGURE 7.

POSITIONING PERFORMANCE

The motion quality of a nanopositioning system is ultimately dependent on the design and performance of a closed-loop controller. In a preliminary effort, this motion system was tested for its point-to-point positioning performance with a lead-lag controller. The steady-state positioning noise was found to be less than 4nm (RMS) over the entire 10mm range of motion (FIGURE 8). In this experiment, the motion stage is actuated in steps of 2.5mm and 20nm (*inset*). These preliminary results show promise for the MMA to be used for large range nanopositioning systems, as it provides bandwidth comparable to VCAs, however with better thermal management and truly non-contact operation, leading to superior positioning performance. Ongoing work includes: **I.**

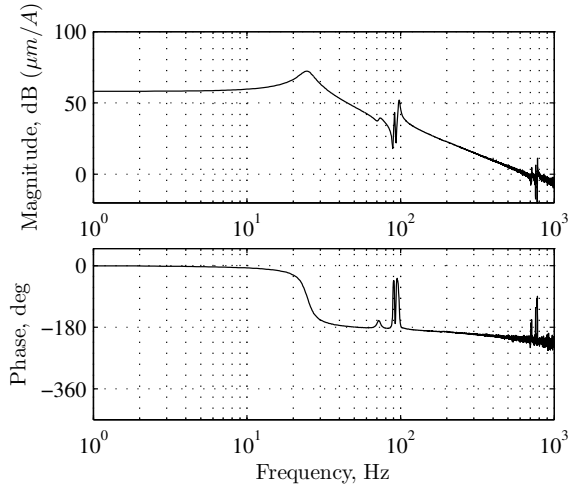

FIGURE 7. Open-Loop Frequency Response.

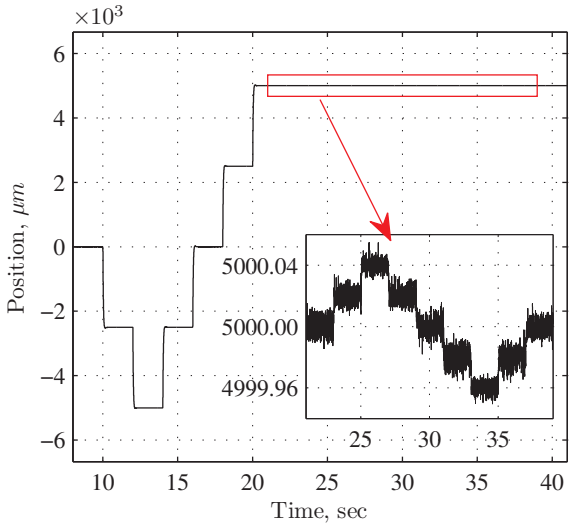

FIGURE 8. Motion Stage Position Response.

Derivation of accurate closed-form models of the MMA's magnetic circuit. **II.** Design of novel MMA configurations with higher values of β to further improve system bandwidth and motion quality.

REFERENCES

[1] Gaoliang, D., et al., 2004, "Metrological large range scanning probe microscope," *Review of Scientific Instruments*, 75(4), pp. 962-969.

[2] O'Brien, W., 2005, "Long-range motion with nanometer precision," *Photonics Spectra*, 39(6), pp. 80-81.

[3] Hubbard, N. B., et al., 2006, "Actuators for micropositioners and nanopositioners," *Applied Mechanics Reviews*, 59(6), pp. 324-334.

[4] Fukada, S., and Nishimura, K., 2007, "Nanometric positioning over a one-millimeter stroke using a flexure guide and electromagnetic linear motor," *International Journal of Precision Engineering and Manufacturing*, 8, pp. 49-53.

[5] Tat Joo, T., et al., 2008, "A flexure-based electromagnetic linear actuator," *Nanotechnology*, 19(31), pp. 315501-315510.

[6] Marcos, T., 2000, "*The straight attraction: part one*," Motion Control Magazine.

[7] Parmar, G., Hiemstra, D.B., Chen, Y., and Awtar, S., 2011, "*A Moving Magnet Actuator for Large Range Nanopositioning*," ASME DSCC Arlington, VA.

[8] Freudenberg, J. S., Looze, D. P., 1988, *Frequency Domain Properties of Scalar and Multivariable Feedback Systems*, Springer-Verlag, Berlin